Vertical WS_2 spin valve with Ohmic property based on Fe_3GeTe_2 electrodes

Ce Hu(胡策), Faguang Yan(闫法光), Yucai Li(李予才), and Kaiyou Wang(王开友)
Citation: Chin. Phys. B, 2021, 30 (**9**): 097505. DOI: 10.1088/1674-1056/ac078b
Journal homepage: http://cpb.iphy.ac.cn; http://iopscience.iop.org/cpb

What follows is a list of articles you may be interested in

Gate-controlled magnetic transitions in Fe_3GeTe_2 with lithium ion conducting glass substrate

Guangyi Chen(陈光毅), Yu Zhang(张玉), Shaomian Qi(齐少勉), and Jian-Hao Chen(陈剑豪)
Chin. Phys. B, 2021, 30 (**9**): 097504. DOI: 10.1088/1674-1056/ac1338

Magnetic dynamics of two-dimensional itinerant ferromagnet Fe_3GeTe_2

Lijun Ni(倪丽君), Zhendong Chen(陈振东), Wei Li(李威), Xianyang Lu(陆显扬), Yu Yan(严羽), Longlong Zhang(张龙龙), Chunjie Yan(晏春杰), Yang Chen(陈阳), Yaoyu Gu(顾耀玉), Yao Li(黎遥), Rong Zhang(张荣), Ya Zhai(翟亚), Ronghua Liu(刘荣华), Yi Yang(杨燚), and Yongbing Xu(徐永兵)
Chin. Phys. B, 2021, 30 (**9**): 097501. DOI: 10.1088/1674-1056/ac0e25

Magnon bands in twisted bilayer honeycomb quantum magnets

Xingchuan Zhu(朱兴川), Huaiming Guo(郭怀明), and Shiping Feng(冯世平)
Chin. Phys. B, 2021, 30 (**7**): 077505. DOI: 10.1088/1674-1056/abeee5

Origin of itinerant ferromagnetism in two-dimensional Fe_3GeTe_2

Xi Chen(陈熙), Zheng-Zhe Lin(林正喆), and Li-Rong Cheng(程丽蓉)
Chin. Phys. B, 2021, 30 (**4**): 047502. DOI: 10.1088/1674-1056/abd164

Evolution of domain structure in Fe_3GeTe_2

Siqi Yin(尹思琪), Le Zhao(赵乐), Cheng Song(宋成), Yuan Huang(黄元), Youdi Gu(顾有地), Ruyi Chen(陈如意), Wenxuan Zhu(朱文轩), Yiming Sun(孙一鸣), Wanjun Jiang(江万军), Xiaozhong Zhang(章晓中), and Feng Pan(潘峰)
Chin. Phys. B, 2021, 30 (**2**): 027505. DOI: 10.1088/1674-1056/abd693

SPECIAL TOPIC — Two-dimensional magnetic materials and devices

Vertical WS_2 spin valve with Ohmic property based on Fe_3GeTe_2 electrodes*

Ce Hu(胡策)[1,2], Faguang Yan(闫法光)[1], Yucai Li(李予才)[1,2], and Kaiyou Wang(王开友)[1,2,3,†]

[1] State Key Laboratory of Superlattices and Microstructures, Institute of Semiconductors, Chinese Academy of Sciences, Beijing 100083, China
[2] Center of Materials Science and Optoelectronics Engineering, University of Chinese Academy of Sciences, Beijing 100049, China
[3] Beijing Academy of Quantum Information Sciences, Beijing 100193, China

(Received 25 February 2021; revised manuscript received 22 March 2021; accepted manuscript online 3 June 2021)

The two-dimensional (2D) transition-metal dichalcogenides (TMDCs) have been recently proposed as a promising class of materials for spintronic applications. Here, we report on the all-2D van der Waals (vdW) heterostructure spin valve device comprising of an exfoliated ultra-thin WS_2 semiconductor acting as the spacer layer and two exfoliated ferromagnetic Fe_3GeTe_2 (FGT) metals acting as ferromagnetic electrodes. The metallic interface rather than Schottky barrier is formed despite the semiconducting nature of WS_2, which could be originated from the strong interface hybridization. The spin valve effect persists up to the Curie temperature of FGT. Moreover, our metallic spin valve devices exhibit robust spin valve effect where the magnetoresistance magnitude does not vary with the applied bias in the measured range up to 50 μA due to the Ohmic property, which is a highly desirable feature for practical application that requires stable device performance. Our work reveals that WS_2-based all-2D magnetic vdW heterostructure, facilitated by combining 2D magnets, is expected to be an attractive candidate for the TMDCs-based spintronic applications.

Keywords: WS_2, Fe_3GeTe_2, spin valve effect, Ohmic property

PACS: 75.70.Cn, 85.75.Bb, 72.25.Mk **DOI:** 10.1088/1674-1056/ac078b

1. Introduction

Two-dimensional (2D) transition-metal dichalcogenides (TMDCs) and their heterostructures have been regarded as a fertile ground for fundamental scientific research and technology application development in the field of solid-state physics.[1,2] Compared with thousands of studies in electronics and optoelectronics, experimental investigations of spintronics based on TMDCs are rare.[3–6] The basic challenge is that the traditional methods to prepare TMDCs-based magnetic heterostructures hinder the acquisition of high-quality electronic interfaces between covalently bonded magnetic materials and ultra-thin van der Waals (vdW) TMDCs layers, which is crucial for spintronic heterostructure devices.[7,8] Encouragingly, the recent discovery of layered magnetic materials could help to overcome this basic challenge.[9–13] The artificial vdW stacking TMDCs-based all-2D magnetic heterostructure in an inert environment through a transfer-stacking method can not only ensure the high-quality interfaces assembled by pristine 2D crystals without degradation, but also avoid the common obstacles in traditional magnetic heterostructure growth such as lattice mismatch and atom interdiffusion.[14,15]

As one of the most studied heterostructure devices in spintronics, vertical spin valve devices are normally composed of two ferromagnetic metals separated by a non-magnetic spacer,[16–20] except for the recent reported spin valve devices using layered ferromagnets without any spacer layer.[21] Despite that there are many reports on the magnetoresistance (MR) effect of spin valve devices with 2D materials (such as graphene) as the nonmagnetic spacer layer, the semiconducting TMDCs-based spin valve remains a relatively unexplored area.[7,22–29] In addition, as distinct from the tunneling spin valve, the low contact resistance and bias-independent MR make the spin valve with Ohmic property more suitable for practical spintronic applications that require stable device performance.[30] Therefore, the TMDCs-based all-2D spin valve with Ohmic property is highly desirable.

Here, we experimentally realized all-2D vertical spin valve devices based on vdW heterostructures comprising of a thin semiconducting WS_2 flake acting as a spacer layer and two exfoliated metallic Fe_3GeTe_2 (FGT) flakes acting as ferromagnetic electrodes. Owing to the influence of the interface hybridization between the ferromagnetic metal FGT and the semiconductor WS_2, we observed Ohmic properties and metallic rather than nonlinear transport behaviors of our FGT/WS_2/FGT spin valve devices. The MR measurements demonstrate that our metallic vdW heterostructure devices have robust spin valve effect where the MR effects do not de-

*Project supported by the National Key R&D Program of China (Grant No. 2017YFA0303400), the National Natural Science Foundation of China (Grant No. 61774144), Beijing Natural Science Foundation Key Program (Grant No. Z190007), and Chinese Academy of Sciences (Grant Nos. QYZDY-SSW-JSC020, XDB44000000, and XDB28000000).

†Corresponding author. E-mail: kywang@semi.ac.cn

pend on the applied bias in the wide range of measurements. And the temperature evolution of the MR effect follows the Bloch's law.

2. Experimental details

Device fabrication The FGT, WS_2, and hexagonal boron nitride (h-BN) (all from HQ Graphene) flakes were mechanically exfoliated inside a nitrogen filled glove box with oxygen and water contents lower than one part-per-million (ppm). Pre-patterned Cr/Au (5/45 nm) electrodes were prepared on Si substrates with 300 nm thickness SiO_2 layer by photolithography, magnetic sputter deposition, and lift-off. Thereafter, vertical FGT/WS_2/FGT/h-BN heterostructures were sequentially transferred and stacked carefully by employing a dry-transfer-stacking method in the glove box. Finally, devices were annealed at 120 °C for 10 min in the glove box to eliminate the possible bubbles and ensure closer stacking between the layers, and were stored inside until the devices were loaded into a low temperature probe station.

Characterizations The magnetotransport measurements were carried out in a cryostat (Lake Shore Cryotronics, Inc) with a base temperature of 10 K and a 2.25 T superconducting magnet. The *I*–*V* curves and spin valve effect were measured by using the combination of a Keithley 2602B SourceMeter and a Keithley 2182A Nanovoltmeter. Note that the positive current direction is defined as the current flow from the top FGT layer to the bottom FGT layer for all devices.

3. Results and discussion

Figure 1(a) shows the schematic diagram of the two-terminal vertical spin valve device, which comprises of two metallic FGT ferromagnetic electrodes separated by a semiconducting WS_2 spacer layer and a top h-BN capping layer. Ultra-thin WS_2 flakes with thickness around 5 nm were used to ensure that the spin polarization of the electron would not be completely scattered when it passes through the WS_2 spacer. The multi-layer FGT flakes with thicknesses exceed 10 nm, which remain a 3D magnetic characteristic, were employed as the ferromagnetic electrodes to guarantee a strong perpendicular magnetic anisotropy and a similar interfacial hybridization strength.[31] The heterostructures were encapsulated with top h-BN layers (typically 20–30 nm) to prevent degradation once exposed to air. Figure 1(b) shows the optical micrograph of the device used to measure the data presented in the main text. The details of the device fabrications and characterizations were given in Section 2. Atomic force microscope (AFM) was applied for the characterization of the device (Fig. S1a). The thicknesses of the layers for a typical vertical heterostructure device were measured as (see Fig. S1b for the height profiles): 13.2 FGT/6.5 WS_2/16.1 FGT/30 h-BN (from bottom to top, in nm).

We first investigated the electrical transport properties of the vertical FGT/WS_2/FGT heterostructure devices from 10 K up to 240 K (above the Curie temperature of FGT), by measuring the current–voltage (*I*–*V*) curves and studying the temperature evolution of the junction resistance (R_{Junction}–*T*). Prior to any charge transport measurements, we first applied a large magnetic field of 0.5 T to ensure the bottom and the top FGT ferromagnetic electrodes in parallel configuration. Figure 2(a) shows that the *I*–*V* curves remain linear at various measured temperatures for both below and above the Curie temperature of FGT, indicating the Ohmic characteristic of the heterostructure device. Moreover, the corresponding R_{Junction}–*T* curve in Fig. 2(b) clearly shows that the R_{Junction} decreases monotonically with decreasing the temperature down to 10 K, revealing the metallic transport behavior of the heterostructure in spite of the semiconducting nature of the WS_2 spacer. Both the linear *I*–*V* characteristic and metallic R_{Junction}–*T* behavior imply the metallic interface rather than the Schottky barriers formed between the WS_2 and the two FGT ferromagnetic electrodes. This is a common behavior of thin semiconductors (such as MoS_2 and WSe_2) sandwiched by ferromagnetic electrodes (such as permalloy and FGT), which originates from the intense hybridization at or in the vicinity of the interfaces.[7,24,26,28]

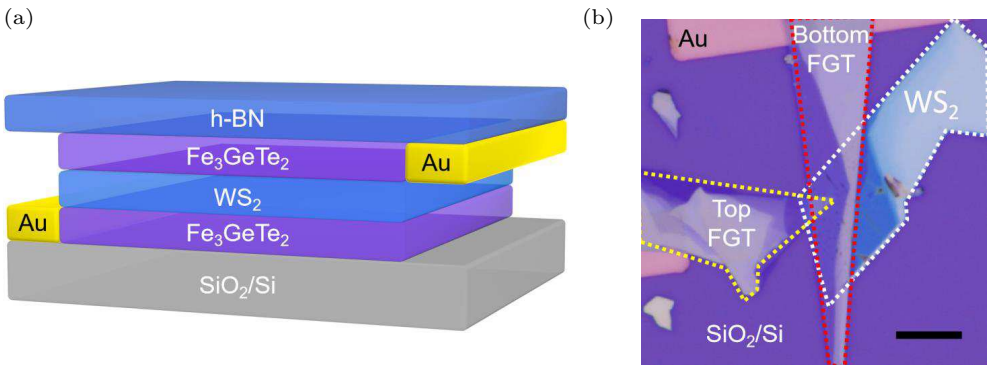

Fig. 1. Device fabrications. (a) Schematic of the FGT/WS_2/FGT vdW heterostructure device, with top h-BN passivation. (b) Optical micrograph of the device used to measure the data presented in the main text (scale bar, 10 μm).

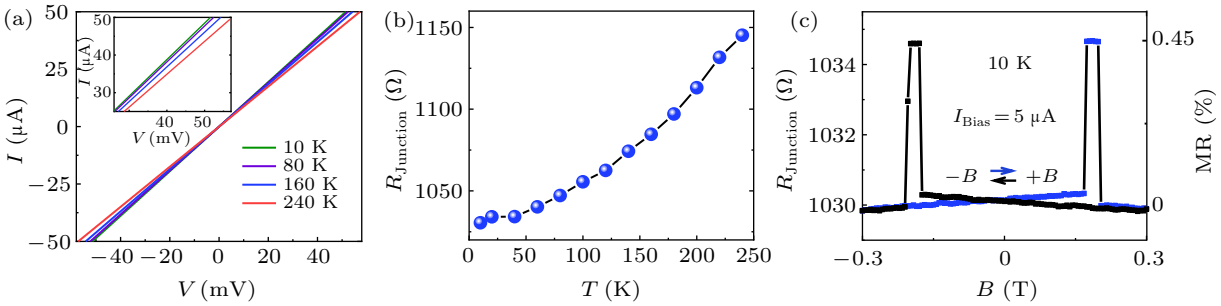

Fig. 2. Magnetotransport properties of the FGT/WS_2/FGT device. (a) *I*–*V* curves at different temperatures, showing the linear characteristics. Inset is the zoom-in view. (b) Resistance of the heterostructure as a function of the temperature ($R_{Junction}$–T). $R_{Junction}$ increases with rising temperature in the measurement range 10 K to 240 K, exhibiting a metallic behavior. (c) Hysteresis of the device resistance as a function of the perpendicular magnetic field ($R_{Junction}$–B) at a fixed current bias of 5 μA. Black and blue horizontal arrows represent the sweeping directions of the magnetic field.

Having known the mechanism of the vertical transport of the WS_2-based heterostructure devices, we then investigated the spin valve effects by measuring the $R_{Junction}$ as a function of the perpendicular magnetic field ($R_{Junction}$–B) at a particular bias current (5 μA, unless otherwise specified). Figure 2(c) shows the $R_{Junction}$–B curves at 10 K, displaying typical spin valve effects with two resistance states. When the magnetic field is swept from negative to positive (blue curves), sharp transition to the high resistance state is observed when the field is close to 0.17 T (corresponding to the antiparallel magnetization alignments ↓↑ or ↑↓, where the arrow represents the out of plane magnetization of the FGT ferromagnetic electrode), and then falls back to the low resistance state (corresponding to the parallel magnetization alignments ↓↓ or ↑↑) at a slightly larger field of around 0.20 T. When the magnetic field is swept back to negative (black curves), the resistance has corresponding symmetric up and down transition. The magnitude of the associated magnetoresistance (MR) can be defined by $(R_{AP}-R_P)/R_P$, where R_{AP} and R_P are the resistances at antiparallel and parallel magnetic configurations of the two FGT ferromagnetic electrodes, respectively. The MR is obtained to be 0.45% at 10 K. If we assume the top and bottom FGT ferromagnetic electrodes have the same electron spin polarization P, the MR can be approximated as $\mathrm{MR} = 2P^2/(1-P^2)$, which is deduced from the modified Julliere's model.[7] Then, the spin polarization of the FGT electrodes is calculated to be $\sim 5\%$.

Figure 3(a) shows the *I*–*V* curves measured at 10 K in the parallel and antiparallel magnetization alignment under zero magnetic field. The slightly different slopes of the two linear *I*–*V* curves demonstrate the nonvolatile characteristic of the two different magnetic configurations. We further investigated the temperature dependence of the spin valve effect. Figure 3 shows the MR curves measured at various temperatures. With increasing the temperature, the magnitude of the MR decreases and vanishes above the Curie temperature at about 220 K, as shown in Figs. 3(b) and 3(c). The reduction of the MR at higher temperatures can be caused by two reasons: one is that the thermal fluctuation strengthens with rising the temperature, and the other is that the spin polarization is proportional to the magnetization and decreases with increasing temperature. Moreover, the critical magnetic switching field of the spin valve decreases with increasing the temperature [Fig. 3(b)], which is attributed to the temperature dependence of the switching fields in the FGT flakes. The coercivity of FGT decreases with increasing the temperature, which is the result of the reduction of perpendicular anisotropic energy and the enhancement of thermal agitation energy.[31] The temperature evolution of the MR magnitude can be analyzed by Bloch's law, where the spin polarization is described by $P(T) = P_0(1-\alpha T^{3/2})$. Thus, by fitting the temperature dependence of the spin polarization, a material-dependent constant α can be estimated to be 1.4×10^{-4} $\mathrm{K}^{-3/2}$. This value is comparable to the reported value in the literature.[28]

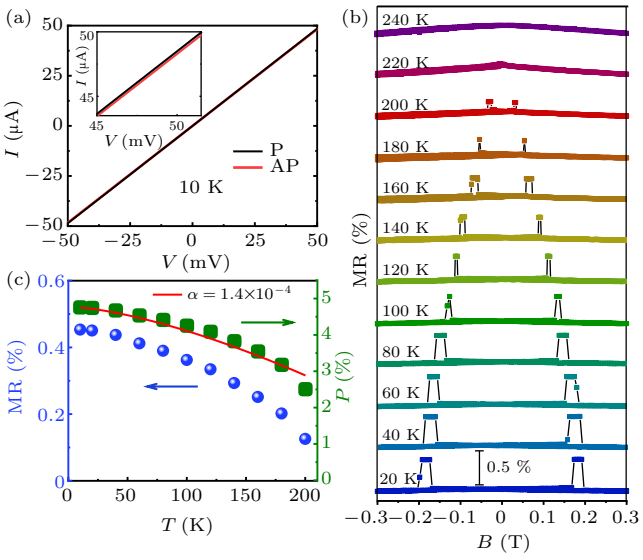

Fig. 3. Temperature-dependent spin valve effect of the FGT/WS_2/FGT device. (a) *I*–*V* curves in parallel (P) and antiparallel (AP) magnetization alignment measured at 10 K under zero magnetic field. Inset is the zoom-in view. (b) MR curves at different temperatures. (c) MR magnitude and the corresponding spin polarization (P) as a function of temperature. The data is fitted to Bloch's law (red line), yielding a material-dependent parameter $\alpha = 1.4\times10^{-4}$ $\mathrm{K}^{-3/2}$.

Next, we studied the bias current dependence of the MR effect at 10 K. As shown in Fig. 4(a), the MR curve measured at a negative bias current of 5 μA yields the value of

0.45%, which is equal to the value of the positive counterpart, implying that the device possesses perfect up-down symmetry and two identical high-quality FGT-WS_2 vdW interfaces. The physical mechanism of our spin valve devices is the spin-dependent scattering transport. Figure 4(b) shows the spin valve effect at various bias currents ranging from 100 nA to 50 μA. As shown in Fig. 4(c), owing to the Ohmic property of the WS_2-based spin valve device, the MR magnitude stabilizes around 0.45% and does not depend on the bias current, which meets the demand in stable device performance for practical spintronic applications. This bias-independent MR behavior was also observed in the previous studies.[30]

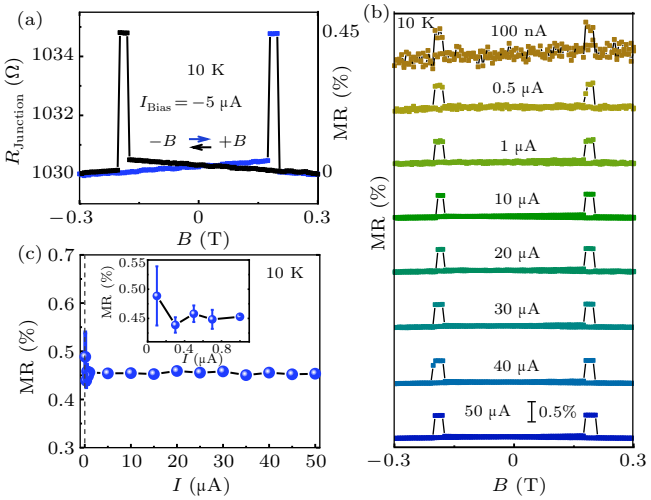

Fig. 4. Bias-dependent spin valve effect. (a) MR curve measured at a negative bias current of 5 μA. (b) MR curves at various bias currents ranging from 100 nA to 50 μA. (c) MR magnitude as a function of bias current. Inset is the zoom-in view.

4. Conclusion

In summary, we have fabricated and investigated spin valve devices with high quality interfaces based on FGT/WS_2/FGT vdW heterostructures. Interestingly, the unexpected Ohmic property and metallic rather than nonlinear transport behaviors were observed. This should be a universal phenomenon of ultrathin semiconductors sandwiched by ferromagnetic electrodes, which is related to the strong hybridization between the interface of WS_2 and FGT. Moreover, the magnetotransport measurements show that our WS_2-based metallic heterostructure devices have robust spin valve effect, and its MR effects do not depend on the bias current due to the Ohmic property. The results of our work indicate that all-2D magnetic heterostructure, facilitated by combining 2D magnets, is expected to be a promising alternative for TMDCs-based spintronics, and may contribute a feasible spin valve structure for realistic applications that require stable device performance.

References

[1] Wang Q H, Kalantar-Zadeh K, Kis A, Coleman J N and Strano M S 2012 *Nat. Nanotech.* **7** 699
[2] Manzeli S, Ovchinnikov D, Pasquier D, Yazyev O V and Kis A 2017 *Nat. Rev. Mater.* **2** 17033
[3] Jariwala D, Sangwan V K, Lauhon L J, Marks T J and Hersam M C 2014 *ACS Nano* **8** 1102
[4] Mak K F and Shan J 2016 *Nat. Photon.* **10** 216
[5] Xu X, Yao W, Xiao D and Heinz T F 2014 *Nat. Phys.* **10** 343
[6] Qian X, Liu J, Fu L and Li J 2014 *Science* **346** 1344
[7] Wang W, Narayan A, Tang L, Dolui K, Liu Y, Yuan X, Jin Y, Wu Y, Rungger I, Sanvito S and Xiu F 2015 *Nano Lett.* **15** 5261
[8] Lin X, Yang W, Wang K L and Zhao W 2019 *Nat. Electron.* **2** 274
[9] Gong C, Li L, Li Z, Ji H, Stern A, Xia Y, Cao T, Bao W, Wang C, Wang Y, Qiu Z Q, Cava R J, Louie S G, Xia J and Zhang X 2017 *Nature* **546** 265
[10] Huang B, Clark G, Navarro-Moratalla E, Klein D R, Cheng R, Seyler K L, Zhong D, Schmidgall E, McGuire M A, Cobden D H, Yao W, Xiao D, Jarillo-Herrero P and Xu X 2017 *Nature* **546** 270
[11] Deng Y, Yu Y, Song Y, Zhang J, Wang N Z, Sun Z, Yi Y, Wu Y, Wu S, Zhu J, Wang J, Chen X and Zhang Y 2018 *Nature* **563** 94
[12] Bonilla M, Kolekar S, Ma Y, Diaz H C, Kalappattil V, Das R, Eggers T, Gutierrez H R, Phan M and Batzill M 2018 *Nat. Nanotech.* **13** 289
[13] Ghazaryan D, Greenaway M T, Wang Z, Guarochico-Moreira V H, Vera-Marun I J, Yin J, Liao Y, Morozov S V, Kristanovski O, Lichtenstein A I, Katsnelson M I, Withers F, Mishchenko A, Eaves L, Geim A K, Novoselov K S and Misra A 2018 *Nat. Electron.* **1** 344
[14] Gong C and Zhang X 2019 *Science* **363** eaav4450
[15] Gibertini M, Koperski M, Morpurgo A F and Novoselov K S 2019 *Nat. Nanotech.* **14** 408
[16] Julliere M 1975 *Phys. Lett. A.* **154** 225
[17] Moodera J S, Kinder L R, Wong T M and Meservey R 1995 *Phys. Rev. Lett.* **74** 3273
[18] Diény B 1994 *J. Magn. Magn. Mater.* **136** 335
[19] Zhou G H, Wang Y G and Qi X J 2009 *Chin. Phys. Lett.* **26** 037501
[20] Qi X J, Wang Y G, Miao X F, Li Z Q and Huang Y Z 2010 *Chin. Phys. B* **19** 037505
[21] Hu C, Zhang D, Yan F, Li Y, Lv Q, Zhu W, Wei Z, Chang K and Wang K 2020 *Sci. Bull.* **65** 1072
[22] Entani S, Seki T, Sakuraba Y, Yamamoto T, Takahashi S, Naramoto H, Takanashi K and Sakai S 2016 *Appl. Phys. Lett.* **109** 082406
[23] Wang Z, Sapkota D, Taniguchi T, Watanabe K, Mandrus D and Morpurgo A F 2018 *Nano Lett.* **18** 4303
[24] Iqbal M Z, Iqbal M W, Siddique S, Khan M F and Ramay S M 2016 *Sci. Rep.* **6** 1
[25] Wu H, Coileáin C, Abid M, Mauit O, Syrlybekov A, Khalid A, Xu H, Gatensby R, Wang J J, Liu H, Yang L, Duesberg G S, Zhang H, Abid M and Shvets I V 2015 *Sci. Rep.* **5** 15984
[26] Zhao K, Xing Y, Han J, Feng J, Shi W, Zhang B and Zeng Z 2017 *J. Magn. Magn. Mater.* **432** 10
[27] Zatko V, Galbiati M, Dubois S M, Och M, Palczynski P, Mattevi C, Brus P, Bezencenet O, Martin M, Servet B, Charlier J, Godel F, Vecchiola A, Bouzehouane K, Collin S, Petroff F, Dlubak B and Seneor P 2019 *ACS Nano* **13** 14468
[28] Lin H, Yan F, Hu C, Lv Q, Zhu W, Wang Z, Wei Z, Chang K and Wang K 2020 *ACS Appl. Mater. & Inter.* **12** 43921
[29] Chen J, Meng J, Zhou Y, Wu H, Bie Y, Liao Z and Yu D 2013 *Nat. Commun.* **4** 1921
[30] Meng J, Chen J J, Yan Y, Yu D P and Liao Z M 2013 *Nanoscale* **5** 8894
[31] Tan C, Lee J, Jung S, Park T, Albarakati S, Partridge J, Field M R, McCulloch D G, Wang L and Lee C 2018 *Nat. Commun.* **9** 1